Effects of rising CO_2 on the harmful cyanobacterium Microcystis

Sandrini, G.

Publication date
2016
Document Version
Final published version

Chapter 2

Genetic diversity of inorganic carbon systems causes variation in CO_2 response of the cyanobacterium *Microcystis*

Genetic diversity of inorganic carbon systems causes variation in CO_2 response of the cyanobacterium *Microcystis*

Giovanni Sandrini, Hans C. P. Matthijs, Jolanda M. H. Verspagen, Gerard Muyzer, Jef Huisman

Department of Aquatic Microbiology, Institute for Biodiversity and Ecosystem Dynamics, University of Amsterdam, Amsterdam, The Netherlands

Keywords: bicarbonate transport; CO_2-concentrating mechanism; climate change; harmful cyanobacteria; *Microcystis aeruginosa*; natural selection

This chapter is published as:
Sandrini G, Matthijs HCP, Verspagen JMH, Muyzer G, Huisman J. (2014). Genetic diversity of inorganic carbon uptake systems causes variation in CO_2 response of the cyanobacterium *Microcystis*. *ISME Journal* **8:** 589–600.

Abstract

Rising CO_2 levels may act as an important selective factor on the CO_2-concentrating mechanism (CCM) of cyanobacteria. We investigated genetic diversity in the CCM of *Microcystis aeruginosa*, a species producing harmful cyanobacterial blooms in many lakes worldwide. All 20 investigated *Microcystis* strains contained complete genes for two CO_2 uptake systems, the ATP-dependent bicarbonate uptake system BCT1 and several carbonic anhydrases (CAs). However, twelve strains lacked either the high-flux bicarbonate transporter BicA or the high-affinity bicarbonate transporter SbtA. Both genes, *bicA* and *sbtA*, were located on the same operon, and the expression of this operon is most likely regulated by an additional LysR-type transcriptional regulator (CcmR2). Strains with only a small *bicA* fragment clustered together in the phylogenetic tree of *sbtAB*, and the *bicA* fragments were similar in strains isolated from different continents. This indicates that a common ancestor may first have lost most of its *bicA* gene and subsequently spread over the world. Growth experiments showed that strains with *sbtA* performed better at low inorganic carbon (C_i) conditions, whereas strains with *bicA* performed better at high C_i conditions. This offers an alternative explanation of previous competition experiments, as our results reveal that the competition at low CO_2 levels was won by a specialist with only *sbtA*, whereas a generalist with both *bicA* and *sbtA* won at high CO_2 levels. Hence, genetic and phenotypic variation in C_i uptake systems provide *Microcystis* with the potential for microevolutionary adaptation to changing CO_2 conditions, with a selective advantage for *bicA*-containing strains in a high-CO_2 world.

Introduction

High nutrient loads can favor the development of dense cyanobacterial blooms (Chorus and Bartram, 1999; Paerl, 2008; Brauer *et al.*, 2012), which increase the turbidity of lakes, deplete night-time oxygen concentrations, suppress the growth of submerged plants and thereby impair important underwater habitat for aquatic invertebrates and fish species (Scheffer, 1998; Gulati and Van Donk, 2002). Moreover, several bloom-forming cyanobacteria produce toxins, causing serious and sometimes fatal liver, digestive and neurological diseases in birds and mammals, including humans (Carmichael, 2001; Cox *et al.*, 2003; Codd *et al.*, 2005). Cyanobacterial blooms are therefore a major threat to the use of lakes for drinking water, irrigation, fishing and recreation (Chorus and Bartram, 1999; Falconer, 2005; Huisman *et al.*, 2005). Although recent studies warn that cyanobacterial blooms may benefit from global warming (Jöhnk *et al.*, 2008; Paerl and Huisman, 2008; Kosten *et al.*, 2012; Michalak *et al.*, 2013), their possible response to rising CO_2 levels remains less clear.

Eutrophic lakes vary widely in the availability of inorganic carbon (C_i). Many lakes are supersaturated with CO_2 due to degradation of organic matter, sometimes resulting in

dissolved CO_2 concentrations exceeding 10,000 ppm (Cole *et al.*, 1994; Sobek *et al.*, 2005; Lazzarino *et al.*, 2009). However, the photosynthetic activity of dense cyanobacterial blooms can strongly deplete the dissolved CO_2 concentration, resulting in severely undersaturated CO_2 conditions (Ibelings and Maberly, 1998; Balmer and Downing, 2011; Gu *et al.*, 2011). CO_2 depletion by dense blooms raises the pH, sometimes even to pH>10.5 (Talling, 1976; Jeppesen *et al.*, 1990; López-Archilla *et al.*, 2004; Verschoor *et al.*, 2013), shifting the C_i balance towards bicarbonate and carbonate.

Cyanobacteria have had a long evolutionary history, during which they have developed highly efficient CO_2-concentrating mechanisms (CCMs) that enable them to grow well at a wide range of C_i conditions (Kaplan and Reinhold, 1999; Giordano *et al.*, 2005; Badger *et al.*, 2006; Price *et al.*, 2008; Raven *et al.*, 2012). The CCMs of cyanobacteria are structurally and phylogenetically different from those of most eukaryotic algae (Raven, 2010; Wang *et al.*, 2011b), and it has been argued that bloomforming cyanobacteria are particularly adept to compete at the low CO_2 and high-pH conditions typical of dense blooms (Shapiro, 1990). Furthermore, several bloom-forming cyanobacterial species are buoyant and can float upwards, which provides an advantage in competition for light (Walsby *et al.*, 1997; Huisman *et al.*, 2004; Jöhnk *et al.*, 2008) and enables surface blooms to intercept the CO_2 influx at the airwater interface (Paerl and Ustach, 1982; Ibelings and Maberly, 1998).

So far, five different C_i uptake systems have been identified in cyanobacteria, two for CO_2 (Shibata *et al.*, 2001) and three for bicarbonate (Omata *et al.*, 1999; Shibata *et al.*, 2002; Price *et al.*, 2004; Price, 2011). These uptake systems have different properties (Price *et al.*, 2004), and not all uptake systems are present in every cyanobacterium (Rae *et al.*, 2011). The CO_2 uptake systems convert CO_2, which has passively diffused into the cell, to bicarbonate in a NADPH-dependent reaction involving NDH-I complexes with specific subunits (Price, 2011). The NDH-I_3 CO_2 uptake system has a high substrate affinity ($K_{0.5}$ = 1-2 mmol L^{-1} CO_2) and low flux rate (Maeda *et al.*, 2002; Price *et al.*, 2002). Conversely, the NDH-I_4 CO_2 uptake system has a lower substrate affinity ($K_{0.5}$ = 10-15 mmol L^{-1} CO_2) but high flux rate (Maeda *et al.*, 2002; Price *et al.*, 2002).

The three bicarbonate uptake systems are located in the plasma membrane (Price, 2011). The first, BicA, has a low substrate affinity ($K_{0.5}$ = 70-350 mmol L^{-1} bicarbonate, depending on the species) but a high flux rate (Price *et al.*, 2004). The second bicarbonate transporter, SbtA, has a high substrate affinity ($K_{0.5}$ < 5 mmol L^{-1} bicarbonate) but low flux rate (Price *et al.*, 2004). Downstream of *sbtA*, another associated gene, *sbtB*, is often found. The function of SbtB is still unknown, and it does not seem essential for SbtA activity (Price, 2011). Both SbtA and BicA are sodium-dependent bicarbonate transporters (Shibata *et al.*, 2002; Price *et al.*, 2004), although the molecular details of their sodium co-transport have not

yet been elucidated (Price and Howitt, 2011; Price *et al.*, 2011b). The third bicarbonate transporter, BCT1, has a high substrate affinity ($K_{0.5}$ = 10-15 mmol L^{-1} bicarbonate) and low flux rate (Omata *et al.*, 2002). It consists of four subunits (CmpABCD) and is directly ATP-dependent (Omata *et al.*, 1999; Price *et al.*, 2008).

In addition, cyanobacteria deploy a variety of CAs (Smith and Ferry, 2000; Badger *et al.*, 2006). This includes periplasmic CAs, such as EcaA (α-type CA) and EcaB (β-type CA), which are thought to convert bicarbonate to CO_2 in the periplasmic space between the outer cell wall and plasma membrane to facilitate carbon transport into the cell (Soltes-Rak *et al.*, 1997; So *et al.*, 1998). The carboxysomal CcaA (β-type CA) converts bicarbonate to CO_2 in the carboxysome, thus enhancing the CO_2/O_2 ratio near the key enzyme RuBisCO to facilitate its CO_2 fixation activity.

In this paper, we analyze the genetic diversity of CCM genes among 20 different strains of the harmful cyanobacterium *Microcystis aeruginosa* (hereafter referred to as *Microcystis*). *Microcystis* is a widespread genus that can produce the toxin microcystin (MC) and develops dense blooms in many eutrophic lakes and brackish waters across the globe (Chen *et al.*, 2003; Orr *et al.*, 2004; Verspagen *et al.*, 2006; Tonk *et al.*, 2007; Paerl and Huisman, 2008; Michalak *et al.*, 2013). Our analysis reveals genetic diversity in the presence/absence of the bicarbonate uptake genes *bicA* and *sbtA* among *Microcystis* strains. Moreover, we show that strains with *sbtA* grow better at low C_i conditions, whereas strains with *bicA* grow better at high C_i conditions. The presence of both genotypic and phenotypic variation in C_i uptake systems indicates that rising CO_2 levels may potentially affect the genetic composition of *Microcystis* blooms.

Results

CCM genes of *Microcystis*

Analysis of the CCM genes of the 20 investigated *Microcystis* strains revealed substantial genetic diversity in the sodium-dependent bicarbonate uptake genes *bicA* and *sbtA* (**Table 2.1**). In total, eight strains contained both *bicA* and *sbtA*, one strain (NIVA-CYA 140) had a transposon inserted in a complete *bicA* gene, ten strains contained a small fragment of *bicA* but lacked a complete *bicA* gene and one strain (PCC 7806) lacked the *sbtAB* genes. Genes encoding the two CO_2 uptake systems NDH-I_3 and NDH-I_4, the ATP-dependent bicarbonate uptake system BCT1 and the three CAs EcaA, EcaB and CcaA were detected in all 20 strains. Strains NIES-843, PCC 9443, PCC 9807 and PCC 9809 contained an additional but somewhat shorter copy of *ccaA*, called *ccaA2*, next to the original gene. We found β-carboxysomal structural genes in all 13 fully sequenced *Microcystis* strains; these were not

further investigated by PCR in the additional seven *Microcystis* strains. There was no relationship between the presence of C_i uptake genes and MC genes (**Table 2.1**).

Table 2.1. The presence of several CCM genes in reference cyanobacteria and the investigated *Microcystis* strains.

Cyanobacterium	Strain origin	C_i uptake systems					Carbonic anhydrases			MC genes
		CO_2		HCO_3^-			α		β	
		NDH-I_3[a]	NDH-I_4[b]	BicA[b]	SbtA[a]	BCT1[a]	EcaA	EcaB	CcaA	
Synechocystis PCC 6803	USA (California)	+	+	2	+	+	−	+	+	−
Synechococcus PCC 7002	PRI (Magueyes Island)	+	+	2	+	−	+	−	+	−
Synechococcus PCC 7942	USA (Texas)	+	+	−	+	+	+	−	+	−
Anabaena ATCC 29413	USA (Mississippi)	+	+	+, ≠	+	+	+	2	+	−
Microcystis CCAP 1450/10[c]	GBR (Lake Blelham Tarn)	+	+	≠	+	+	+	+	+	+
Microcystis CCAP 1450/11[c]	JPN (Tokyo)	+	+	≠	+	+	+	+	+	−
Microcystis HUB 5-2-4[c]	DEU (Lake Pehlitzsee)	+	+	≠	+	+	+	+	+	+
Microcystis HUB 5-3[c]	DEU (Lake Pehlitzsee)	+	+	+	+	+	+	+	+	−
Microcystis NIES-843	JPN (Lake Kasumigaura)	+	+	≠	+	+	+	+	2	+
Microcystis NIVA-CYA 140[c]	CAN (Lake Bruno)	+	+	#	+	+	+	+	+	+
Microcystis PCC 7005	USA (Lake Mendota)	+	+	+	+	+	+	+	+	−
*Microcystis*PCC 7806	NLD (Braakman)	+	+	+	−	+	+	+	+	+
Microcystis PCC 7941	CAN (Little Rideau Lake)	+	+	+	+	+	+	+	+	+
Microcystis PCC 9432	CAN (Little Rideau Lake)	+	+	+	+	+	+	+	+	−
Microcystis PCC 9443	CAF	+	+	≠	+	+	+	+	2	+
Microcystis PCC 9701	FRA (Guerlesquin dam)	+	+	≠	+	+	+	+	+	−
Microcystis PCC 9717	FRA (Rochereau dam)	+	+	≠	+	+	+	+	+	−
Microcystis PCC 9806	USA (Oshkosh)	+	+	+	+	+	+	+	+	−
Microcystis PCC 9807	ZAF (Hartbeespoort dam)	+	+	+	+	+	+	+	2	+
Microcystis PCC 9808	AUS (Malpas dam)	+	+	≠	+	+	+	+	+	+
Microcystis PCC 9809	USA (Lake Michigan)	+	+	+	+	+	+	+	2	+
Microcystis T1-4	THA (Bangkok)	+	+	≠	+	+	+	+	+	−
Microcystis V145[c]	NLD (Lake Volkerak)	+	+	+	+	+	+	+	+	−
Microcystis V163[c]	NLD (Lake Volkerak)	+	+	≠	+	+	+	+	+	+

+, the gene is present, −, the gene is absent, ≠, only a small fragment of the gene is present; #, the gene is complete but disrupted by a transposon; 2, the genome contains two copies of the gene. The origins of the strains are indicated with three-letter codes of the different countries (ISO 3166-1 α-3). The presence of CCM genes is based on high similarity with the reference genes in *Synechocystis* PCC 6803 or *Synechococcus* PCC 7942. The presence of microcystin (MC) genes indicates potentially toxic strains.

[a]C_i uptake system with a high substrate affinity and low flux rate.

[b]C_i uptake system with a low substrate affinity and high flux rate.

[c]For these strains, results are based on PCR product detection with primers for the concerned gene; PCR products of *bicA* and *sbtA* of these *Microcystis* strains were sequenced.

Variation in sodium-dependent bicarbonate uptake genes

Whenever present, *bicA* and *sbtA* were located in the same genomic region and were flanked by two genes encoding a LysR-type transcriptional regulator and a sodium/proton antiporter NhaS3, which most likely removes sodium imported by the sodium-dependent bicarbonate uptake systems. We distinguished three genotypes (**Figure 2.1**): genotype I contains *bicA* without *sbtAB*, genotype II contains *sbtAB* without (complete) *bicA* and genotype III contains both *bicA* and *sbtAB*. The three genotypes were further subdivided depending on differences in intergenic sequences and the presence of *bicA* fragments or transposons. Strain PCC 9443 was not included in **Figure 2.1**, because part of its sequence data between the *bicA* fragment and *sbtA* are missing but most likely this strain has genotype IIB or IIC.

Transcript analysis showed that *bicA*, *sbtAB* and the sodium/proton antiporter gene *nhaS3* were co-transcribed (see Supplementary Information), which indicates that they are probably located on the same operon. The upstream LysR-type transcriptional regulator gene (in reverse orientation) has thus far not been described for other cyanobacteria but appeared to be very similar to *ccmR*, which encodes for the transcriptional regulator of another CCM gene domain with the high-affinity CO_2 uptake genes. Therefore, we have called it *ccmR2* and it is anticipated to regulate the transcription of the *bicA-sbtAB-nhaS3* operon. An amino acid alignment revealed high similarities between the different CcmR-like transcriptional regulators in *Microcystis* (see Supplementary Information for details). There was some variation in CcmR2 between different strains, especially at the C-terminus. However, we did not find a relation between the C_i uptake genotypes and the sequence of CcmR2.

Phylogenetic analysis of *bicA* and *sbtAB*

Phylogenetic trees were constructed on the basis of the DNA sequences of *bicA* and *sbtAB* (**Figure 2.1**). The strains showed more variation in *sbtAB* than in *bicA*. Clustering of the strains in the phylogenetic tree of *sbtAB* was largely based on the presence or absence of *bicA*. An exception was HUB 5-2-4, which lacked *bicA* but clustered with the strains containing both *sbtAB* and *bicA*. In addition, strain PCC 9806 and three strains from Africa and Australia formed outgroups. Strains that were toxic or isolated from proximate locations did not group together in the phylogenetic trees. Yet, there seems to be some large-scale biogeographical pattern, as all the six North-American strains contained both *sbtAB* and *bicA* (but with a transposon insert in *bicA* of NIVA-CYA 140), whereas all the three Asian strains lacked a complete *bicA*. Strains from Europe included both genotypes.

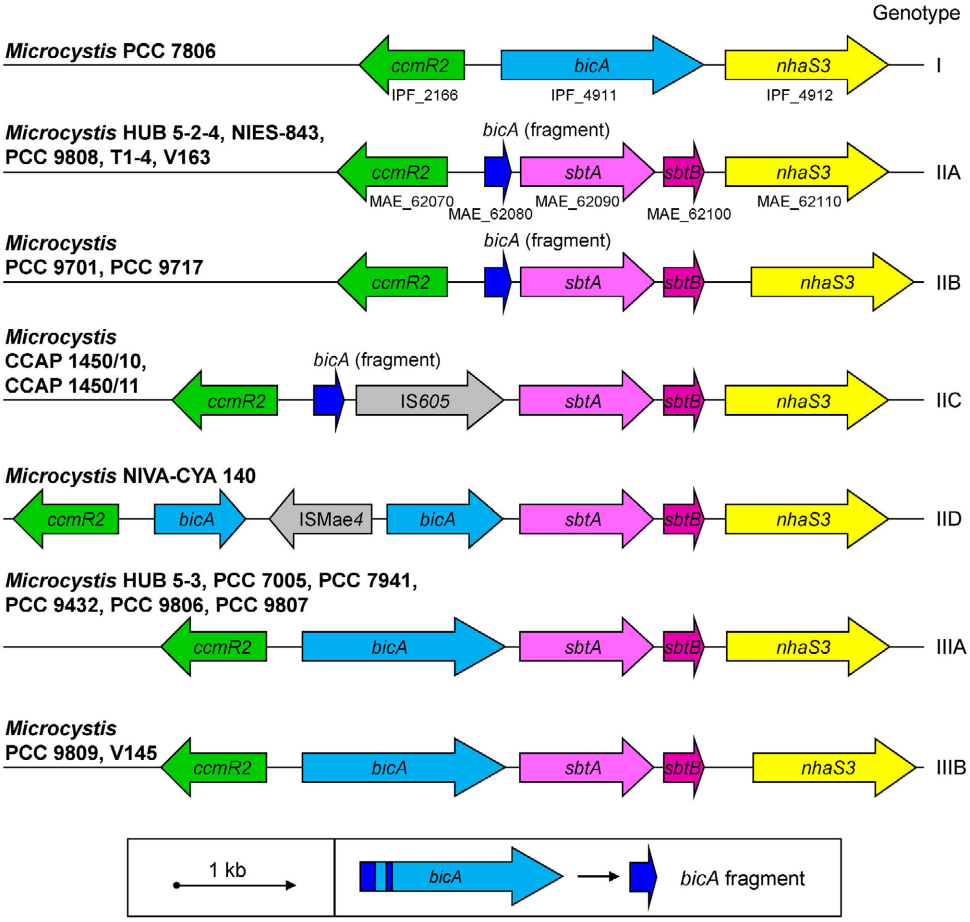

Figure 2.1. Variation of the sodium-dependent bicarbonate uptake genomic region in different *Microcystis* strains. The genomic regions contain the sodium-dependent bicarbonate uptake genes (*bicA* and *sbtAB*) and adjacent genes encoding a transcriptional regulator (*ccmR2*) and a sodium/proton antiporter (*nhaS3*). Several strains lack a complete *bicA* but have a *bicA* fragment consisting of two parts of the 50-end of *bicA* (indicated in the bottom panel). NIVA-CYA 140 has a defective *bicA* gene caused by a transposon insertion (ISMae*4*). CCAP 1450/10 and 1450/11 have a transposon insert (IS*605*) next to a *bicA* fragment. Adjacent genes upstream of ccmR2 are CP12 (Calvin–Benson cycle protein) or *ftsH* (cell division factor). Adjacent genes downstream of *nhaS3* include a gene encoding a N6amt1 (N6-adenine-specific DNA methyltransferase type I) protein, a gene encoding a 2-hydroxy-6-oxohepta-2,4-dienoate hydrolase and hypothetical genes. The IPF numbers are the locus tags of PCC 7806, and the MAE numbers are the locus tags of NIES-843. The size marker indicates 1 kb.

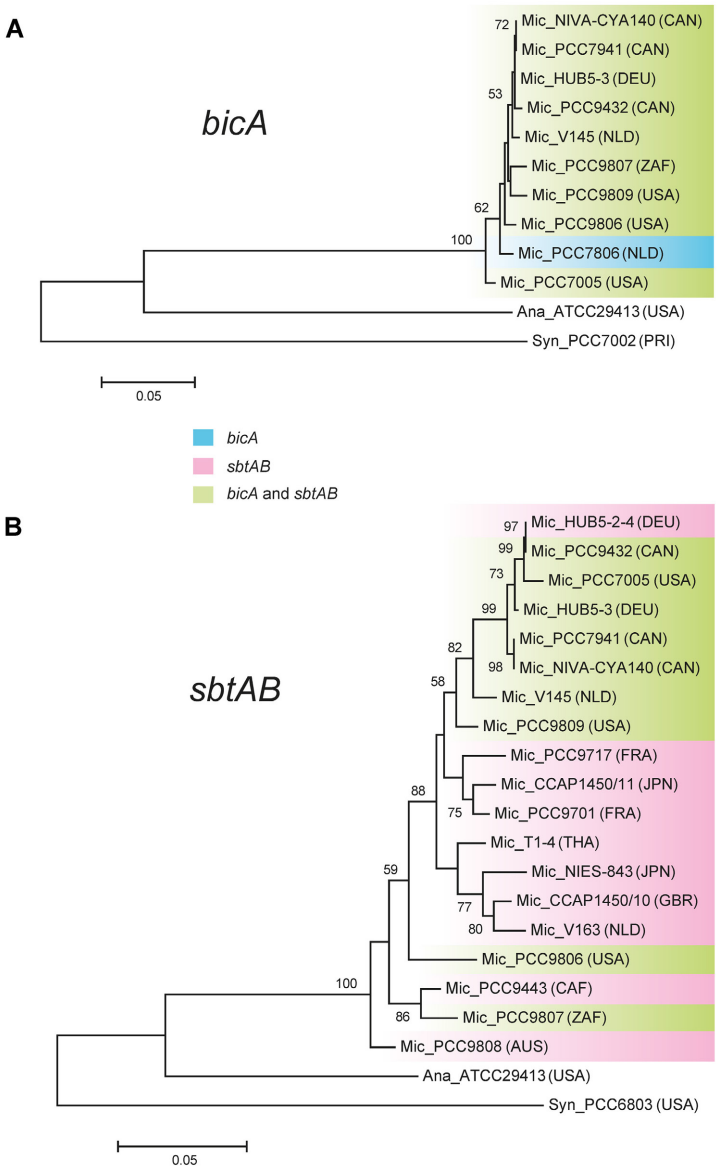

Figure 2.2. Phylogenetic trees of the sodium-dependent bicarbonate uptake genes of *Microcystis*. (A) Phylogenetic tree based on the *bicA* sequences. The outgroup cyanobacteria are *Anabaena variabilis* ATCC 29413 and *Synechococcus* PCC 7002, which both have complete *bicA*. **(B)** Phylogenetic tree based on the *sbtAB* sequences. The outgroup cyanobacteria are *Anabaena variabilis* ATCC 29413 and *Synechocystis* PCC 6803, which both have complete *sbtAB*. Color coding indicates the presence of *bicA* and *sbtAB* in the different *Microcystis* strains. The origin of the strains is shown with three-letter codes indicating the different countries (ISO 3166-1 α-3). The NIVA-CYA 140 *bicA* sequence consists of the two parts originally separated by a transposon insert (Figure 2.1). Bootstrap values (1,000 replicates) are shown for confidence levels higher than 50%. The scale bars indicate the number of nucleotide substitutions per site.

Growth experiments

In the growth experiments, higher CO_2 levels in the gas flow yielded higher concentrations of dissolved CO_2 (**Figure 2.3A**), higher bicarbonate concentrations (**Figure 2.3B**) and a lower pH (**Figure 2.3C**) in the mineral medium. The addition of CAPSO buffer increased the alkalinity, which resulted in a higher bicarbonate concentration and in a higher pH at 400 and 10,000 ppm CO_2. The specific growth rate of strain PCC 7806, which contained *bicA* but lacked *sbtA*, was significantly reduced at the lowest CO_2 level of 20 ppm, especially in the absence of the CAPSO buffer (**Figure 2.4A; Table S2.3, Supplementary Information**). Addition of CAPSO buffer at 20 ppm CO_2 increased the bicarbonate concentration and significantly improved the growth rate of PCC 7806, although it remained below the growth rates at 400 and 10,000 ppm CO_2. The PCC 7806 Δ*mcyB* mutant responded similarly as the wild type, indicating that MC production had little or no effect on the CO_2 response in this study (**Figure 2.4B**). Strain PCC 7005, which contained both *bicA* and *sbtA*, maintained a high growth rate irrespective of the applied CO_2 level and CAPSO buffer (**Figure 2.4C**). The growth rate of strain NIES-843, which contained *sbtA* but lacked a complete bicA gene, was significantly reduced at the highest CO_2 level of 10,000 ppm, especially in the absence of CAPSO buffer (**Figure 2.4D**). Addition of CAPSO buffer at 10,000 ppm CO_2 significantly improved the growth rate of NIES-843, although it remained below the growth rates at 20 and 400 ppm CO_2.

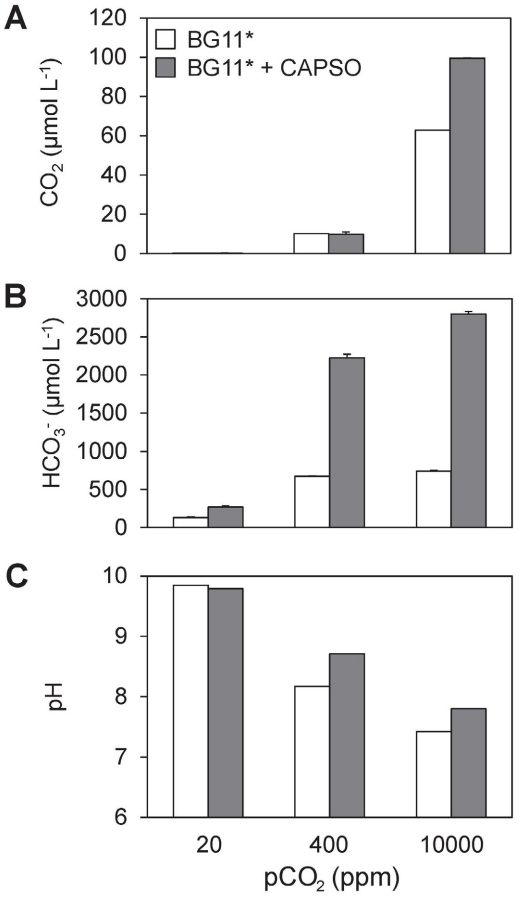

Figure 2.3. Dissolved C_i and pH in the growth experiments. (A) Dissolved CO_2 concentration, **(B)** bicarbonate concentration and **(C)** pH in growth experiments with strain PCC 7005 in sixwell microplates after 1 day of incubation. Dissolved CO_2 and bicarbonate concentrations were calculated from measurements of pH and DIC in the combined supernatant of three biological replicates. Error bars in (A) and (B) represent the standard deviation on the basis of 3-5 repeated measurements in the combined supernatant.

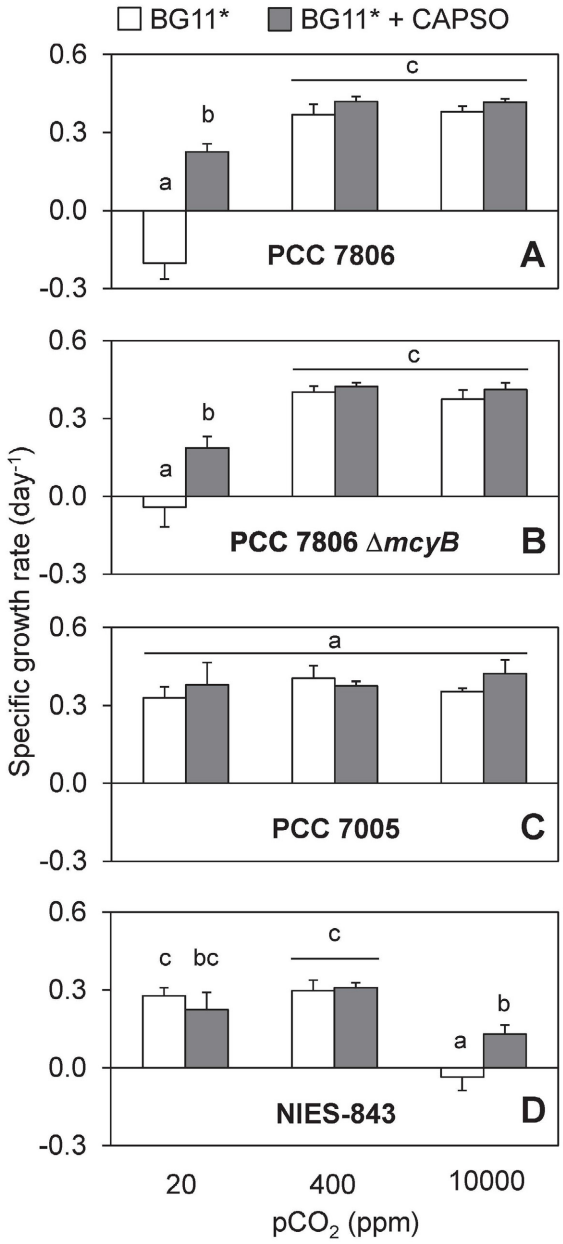

Figure 2.4. Specific growth rates of *Microcystis* strains representative of the three different C_i genotypes at different CO_2 levels. (A) Strain PCC 7806, which contains only *bicA*, **(B)** the mutant strain PCC 7806 Δ*mcyB*, which contains only *bicA* and lacks MC production, **(C)** strain PCC 7005, which contains both *bicA* and *sbtA* and **(D)** strain NIES-843, which contains only *sbtA*. Error bars indicate the standard deviation of 3-6 biological replicates. For each strain, bars with different letters indicate significant differences in growth rate, as tested by a two-way analysis of variance with *post hoc* comparison of the means (see Supplementary Information for details).

Discussion

CCM genes of *Microcystis*

Our results show genetic diversity among the C_i uptake systems of *Microcystis*. In particular, the presence of the sodium-dependent bicarbonate uptake genes *bicA* and *sbtA* varied among the strains, which confirms an earlier suggestion that *Microcystis* strains might differ in their bicarbonate uptake systems (Bañares-España *et al.*, 2006). We found eight strains with both *bicA* and *sbtA*, eleven strains with a small fragment or a defected *bicA* but the complete *sbtA*, whereas one strain had a complete *bicA* but lacked *sbtA*.

On the basis of the available sequencing data, other cyanobacterial species containing both *bicA* and *sbtA* seem to have these genes located in different genomic regions. However, *Microcystis* showed a common genome domain for *bicA*, *sbtA*, *sbtB* and the sodium/proton antiporter gene *nhaS3* (**Figure 2.1**). Transcript analysis revealed that these genes were co-transcribed (see Supplementary Information). Hence, to our knowledge, *Microcystis* is the first example of a cyanobacterium in which *bicA* and *sbtA* are located on the same operon. The presence of a sodium/proton antiporter gene on the same operon strengthens the hypothesis (Shibata *et al.*, 2002; Price *et al.*, 2004) that bicarbonate transport by BicA and SbtA is sodium-dependent. The presence of an upstream LysR-type transcriptional regulator gene, *ccmR2*, makes it likely that transcription of the *bicA-sbtAB-nhaS3* operon is strongly regulated and dependent on environmental conditions.

Genes encoding the two CO_2 uptake systems, NDH-I_3 and NDH-I_4, were present in all 20 investigated *Microcystis* strains. Hence, our results support earlier suggestions (Price *et al.*, 2008; Rae *et al.*, 2011) that both CO_2 uptake systems are widespread among freshwater cyanobacteria. Similarly, all 20 *Microcystis* strains contained the *cmpABCD* genes encoding the bicarbonate uptake system BCT1. We did not find genes with homology to the transcriptional regulator gene *cmpR* of *Synechocystis* and *Synechococcus* in any of the 20 *Microcystis* strains (see Supplementary Information). Most likely, however, the expression of the *cmpABCD* operon and the high-affinity CO_2 operon are strongly regulated, as we detected potential LysR transcriptional regulator binding sites near the most likely -10 TSS of both operons, and found the LysR transcriptional regulator gene *ccmR* upstream of the high-affinity CO_2 operon.

It has been suggested that the two periplasmic CAs, EcaA and EcaB, are not widespread among cyanobacteria (Badger *et al.*, 2006) and do not have an essential role in the CCM of cyanobacteria (So *et al.*, 1998). However, we found both periplasmic CA genes in all 20 *Microcystis* strains. Similarly, Wu *et al.* (2011b) detected transcripts of both *ecaA* and *ecaB* in all their eight *Microcystis* strains from Chinese lakes. Hence, at least in *Microcystis*, these periplasmic CAs are very common.

The carboxysomal CA, CcaA contributes to the delivery of CO_2 to RuBisCO and hence has an important role in the CCM of cyanobacteria (So *et al.*, 1998). Indeed, *ccaA* was present in all our 20 strains as well as the eight *Microcystis* strains investigated by Wu *et al.* (2011b). Only four of our 20 strains contained both *ccaA* and *ccaA2*. The amino-acid sequence of CcaA2 is slightly shorter than CcaA, and the two different isoforms might enable cells to modify their CO_2 fixation efficiency (Long *et al.*, 2007), although further confirmation of this hypothesis is warranted.

Phylogenetic analysis of *bicA* and *sbtAB*

European and Asian strains with a complete *sbtAB* but only a *bicA* fragment clustered together in the phylogenetic tree of *sbtAB* (**Figure 2.2**). It is therefore likely that their ancestors first lost a large part of *bicA* and subsequently spread over the world. Other evidence for a common *bicA* history is that the detected small *bicA* fragments were very similar in these Eurasian strains, the African strain PCC 9443 and the Australian strain PCC 9808. The *bicA* fragments consisted of two short sequences at the 5'-end part of *bicA* (inset in **Figure 1**), whereas the area missing in between has the HIP1 sequences (5'-CGATCG-3') at the outer ends, which have been associated with early gene deletion events (Robinson *et al.*, 1995, 1997). One exception was HUB 5-2-4, which contained the same *bicA* fragment but clustered together in the *sbtAB* tree with strains that had complete *bicA*. Both the *sbtAB* and *nhaS3* genes of HUB 5-2-4 were very similar to PCC 9432. Possibly HUB 5-2-4 acquired these two genes from a recombination event with PCC 9432 or closely related strain, because other gene sequences (*cpcBA*, *ccmR2*) of HUB 5-2-4 and PCC 9432 were less similar.

At first sight, clustering in the phylogenetic trees shows little relationship with the geographical locations from which the strains were collected (**Figure 2.2**). This is in agreement with Janse *et al.* (2004) and Van Gremberghe *et al.* (2011), who did not find a relationship between the rDNA internal-transcribed spacer sequences of *Microcystis* strains and their geographical location, suggesting global dispersal of *Microcystis* strains. However, our six North-American strains contained both *sbtAB* and *bicA* (with a transposon insert in *bicA* of NIVA-CYA 140), the three Asian strains lacked complete *bicA*, strains from Europe included both genotypes and the three strains from Africa and Australia formed outgroups in the *sbtAB* tree. Further studies will be required to verify and explain such possible biogeographical differences.

Growth under different C_i conditions

Our growth experiments support earlier evidence that the sodium-dependent bicarbonate uptake systems BicA and SbtA can have a major impact on cyanobacterial growth (Shibata *et*

al., 2002; Xu *et al.*, 2008). Strains PCC 7005 and NIES-843 both contained the high-affinity but low-flux bicarbonate uptake system SbtA. They grew well at 20 ppm CO_2, presumably because SbtA enabled them to make use of low bicarbonate availability. In contrast, strain PCC 7806 lacked SbtA and was unable to reach a positive growth rate at 20 ppm CO_2 in the absence of CAPSO. Addition of CAPSO buffer at 20 ppm CO_2 increased the bicarbonate concentration (**Figure 2.3B**) and thereby enhanced the growth rate of PCC 7806.

Strain PCC 7806 did contain the ATP-dependent bicarbonate uptake system BCT1, which has a high affinity for bicarbonate. Apparently, the presence of BCT1 could not compensate for the lack of SbtA. This supports the view, based on mutants without a functional BCT1, that BCT1 most likely has a minor role in C_i uptake (Shibata *et al.*, 2002). However, an alternative explanation might be that the relatively high sodium concentration in our growth experiments may have favored the sodium-dependent bicarbonate transporters relative to BCT1. As *Microcystis* occur in both freshwater and brackish environments (Tonk *et al.*, 2007), it would be interesting to further investigate the role of sodium in the bicarbonate uptake of *Microcystis* in detail.

Strains PCC 7806 and PCC 7005 both contained the low-affinity but high-flux bicarbonate uptake system BicA. They grew equally well at 400 and 10,000 ppm CO_2, despite the differences in pH generated by the two applied CO_2 concentrations. BicA most likely enabled them to profit from the high bicarbonate concentrations. In contrast, strain NIES-843 lacked BicA and showed impaired growth at 10,000 ppm CO_2. Possibly, this very high CO_2 level reduced its *sbtA* expression, which may have negative effects on growth when *bicA* is lacking. It might also be that the high CO_2 level reduced the pH to such an extent (**Figure 2.3C**) that the growth rate of NIES-843 was negatively affected, because some *Microcystis* strains are sensitive to pH<8 (Wang *et al.*, 2011a). Addition of CAPSO buffer raised the pH and improved the growth of NIES-843 at 10,000 ppm CO_2.

Our results show that *Microcystis* strains that produce both BicA and SbtA, such as strain PCC 7005, are most versatile in their growth response to different C_i conditions. Hence, why would several strains have lost *bicA* while some others lack *sbtA*? Possibly, the production of two partially redundant bicarbonate transporters is relatively costly, giving a selective disadvantage when only one of the two transporters is needed. If so, C_i uptake generalists (with both *bicA* and *sbtA*) are expected to lose the competition against high-affinity specialists (only *sbtA*) at low C_i conditions and against high-flux specialists (only *bicA*) at high C_i conditions.

Microcystis blooms and rising CO_2

Interestingly, our results reveal that *Microcystis* blooms may consist of mixtures of strains with different C_i uptake systems. Strains V145 and V163 were isolated from the same *Microcystis*

bloom in Lake Volkerak, the Netherlands (Kardinaal *et al.*, 2007). However, although strain V145 contained all five C_i uptake systems, strain V163 lacked a complete *bicA* (**Table 2.1**). Similarly, strains HUB 5-2-4 and HUB 5-3 were isolated from the same *Microcystis* bloom in Lake Pehlitzsee, Germany (Schwabe *et al.*, 1988), but strain HUB 5-3 contained all five C_i uptake systems, whereas strain HUB 5-2-4 lacked *bicA*.

Genetic variation in C_i uptake systems may offer an important template for natural selection. During the development of cyanobacterial blooms, the amount of C_i available per cell is often gradually reduced, which may ultimately result in severely C_i-depleted conditions with a high pH (Ibelings and Maberly, 1998; Balmer and Downing, 2011). This might shift the selective advantage towards strains with *sbtA*, which perform better at low C_i conditions than strains lacking *sbtA* (**Figure 2.4**). Similarly, the evolutionary loss of *bicA* in several *Microcystis* strains might be explained by natural selection during periods of low C_i availability. Conversely, rising atmospheric CO_2 concentrations may enhance the C_i availability in lakes, alleviating cyanobacterial blooms from carbon limitation (Schippers *et al.*, 2004). This would disfavor high-affinity C_i uptake systems (Collins *et al.*, 2006), whereas strains with *bicA* will have a selective advantage in a high-CO_2 world.

These hypotheses are at least partially confirmed by the recent competition experiments of Van de Waal *et al.* (2011) highlighted by Wilhelm and Boyer (2011). They found that the toxic *Microcystis* strain NIVA-CYA 140 displaced the non-toxic strain NIVA-CYA 43 (=PCC 7005) at low CO_2 conditions, whereas the outcome of competition was reversed at high CO_2 conditions. On the basis of additional experiments with *Microcystis* PCC 7806 and its non-MC-producing mutant, Van de Waal *et al.* (2011) explained their results by differences in MC production between the strains, implicating that MCs might have a role in carbon assimilation (see also Zilliges *et al.*, 2011). However, in our study, we did not find an association between C_i uptake genotypes and MC genes. Furthermore, we did not find differences in CO_2 response between the MC-producing wild-type PCC 7806 and its non-MC-producing mutant. Instead, our findings suggest that the results of Van de Waal *et al.* (2011) can be more parsimoniously explained as a shift in competitive dominance from a high-affinity specialist with only *sbtA* (NIVA-CYA 140) at low CO_2 levels to a C_i uptake generalist with *bicA* and *sbtA* (PCC 7005) at high CO_2 levels.

Some words of caution are in place for the extrapolation of these laboratory results to natural field conditions. Our laboratory experiments and the competition studies of Van de Waal *et al.* (2011) were designed to investigate effects of different C_i conditions. We used relatively low light levels, whereas in reality *Microcystis* often performs vertical migrations during blooms, experiencing light conditions ranging from near-zero light levels deeper down in the water column to high light levels of 1,500–2,000 mmol photons m^{-2} s^{-1} at the water

surface (Visser *et al.*, 1997; Wallace *et al.*, 2000). Furthermore, in the real world, bloomforming cyanobacteria compete not only with each other but also with numerous eukaryotic algal species, and their competitive success depends on a multitude of environmental factors including nutrient and light availability, temperature, turbulence, residence time, grazing and viruses (Dokulil and Teubner, 2000; Huisman *et al.*, 2005; Jöhnk *et al.*, 2008; Paerl, 2008). Yet, bloom-forming cyanobacteria do experience extensive variation in environmental C_i concentrations, including strong CO_2 depletion during dense blooms. The presence of genetic and phenotypic variation in C_i uptake systems of *Microcystis* is therefore likely to be of ecological relevance. Hence, our laboratory results clearly call for field studies investigating changes in gene expression and genotype composition of the C_i uptake systems during cyanobacterial bloom development.

In conclusion, we found genetic variation in the C_i uptake systems of *Microcystis* that was reflected by phenotypic variation in CO_2 response and that explained the selection of strains with different C_i uptake strategies at different CO_2 levels. These laboratory results indicate that rising atmospheric CO_2 levels may in potential induce changes in the genotype composition of *Microcystis*, one of the major bloom-forming cyanobacteria threatening the water quality of many lakes and estuaries worldwide. Future field studies may wish to investigate whether and to what extent this potential for microevolutionary change is realized.

Materials and Methods

Genome sequences

We investigated the CCM genes of 20 strains of *M. aeruginosa* (Kützing) (*sensu* Otsuka *et al.*, 2001). Our analysis comprised twelve strains for which the full genome was sequenced in previous studies, including *Microcystis* NIES-843 (Kaneko *et al.*, 2007), *Microcystis* PCC 7806 (Frangeul *et al.*, 2008) and ten *Microcystis* strains recently sequenced by Humbert *et al.* (2013).

In addition, we sequenced the entire genome of *Microcystis* PCC 7005 with the Illumina GAIIx platform (Baseclear, Leiden, the Netherlands). Paired-end sequencing was used with an insert size of 250 bp and a read length of 2x50 bp. This resulted in 27,800,092 reads, of which 94% was assembled with CLC bio's software version 4.7.2 into 1363 contigs with a total length of 4.9 Mb. The large number of contigs is due to many repeats and transposons, which are far more abundant in *Microcystis* than in most other cyanobacteria (Lin *et al.*, 2011). This whole-genome shotgun sequencing project has been deposited at GenBank under the accession AQPY00000000. The version described in this paper is the first version, AQPY01000000.

We applied Blast (Altschul *et al.*, 1990) to search for CCM genes in the twelve previously sequenced *Microcystis* strains, using CCM gene sequences of *Synechocystis* PCC 6803

and *Synechococcus* PCC 7942 as reference. The genomic sequence data of strain PCC 7005 was investigated manually, using the CCM gene sequences of the other *Microcystis* strains as reference.

PCR analysis of additional strains

To enlarge our data set, we developed a series of PCR primers on the basis of the available genome sequences, to investigate the presence of specific CCM genes in seven additional *Microcystis* strains (CCAP 1450/10, CCAP 1450/11, HUB 5-2-4, HUB 5-3, NIVA-CYA 140, V145 and V163). The strains were maintained in our culture collection, using Erlenmeyer flasks incubated at 20°C in BG11 medium (Rippka *et al.*, 1979) at ambient CO_2 and continuous light (~3 mmol photons m^{-2} s^{-1}). Samples for DNA isolation were pelleted by centrifugation (8,000 *g*, 10 min at 20°C). After five freezethawing cycles in liquid N_2 and at 65°C, the DNeasy Blood & Tissue kit (Qiagen GmbH, Hilden, Germany) was used to isolate total DNA according to the instructions for Gram-negative bacteria provided by the supplier.

PCR reactions to detect the presence of CCM genes were performed with the GoTaq® DNA polymerase kit (Promega GmbH, Mannheim, Germany) according to the instructions of the supplier. The sequences of the new primers are listed in the Supplementary Information. The annealing temperature was 56°C. Gel electrophoresis with ethidium bromide staining was used to analyze the PCR products. Selected PCR products of the sodium-dependent bicarbonate transporter genomic region in the seven *Microcystis* strains were sequenced by long run Quick Shot sequencing on an Applied Biosystems 3730XL sequencer (Baseclear). The sequence data were manually checked with the software program Chromas Lite, and overlapping sequences were combined. Most parts were sequenced in both directions. The sequences have been deposited in Genbank and are available under the following accession numbers: KC896021-KC896027.

Comparison of sequence data

The CCM gene sequences of the 20 investigated *Microcystis* strains were aligned with ClustalW version 2.1 (Thompson *et al.*, 1994) to investigate variation in transcription and translation potential as well as phylogenetic relationships among the different genotypes. Possible LysR transcriptional regulator binding sites were defined as TNA-$N_{7/8}$-TNA (Shively *et al.*, 1998; Woodger *et al.*, 2007; Nishimura *et al.*, 2008). The most likely -10 transcriptional start site was based on *Synechocystis* PCC 6803 data, most commonly 5'-TAAAAT-3' (Mitschke *et al.*, 2011). Maximum likelihood phylogenetic trees of *bicA* and *sbtAB* were constructed with the software program MEGA version 5.05 (Tamura *et al.*, 2011) using 1,000 bootstrap replicates.

Growth experiments

We investigated the specific growth rates of axenic strains of *Microcystis* NIES-843, PCC 7005 and PCC 7806, which represented three contrasting C_i uptake genotypes, in different C_i environments. A mutant of PCC 7806, incapable of MC production (PCC 7806 Δ*mcyB*; Dittmann *et al.*, 1997), was also tested to investigate possible effects of MC production. The experimental treatments comprised three different CO_2 levels in the gas flow (20±1, 400±20 and 10,000±400 ppm), with or without the addition of an alkaline buffer solution (5 mM CAPSO-NaOH, pH 10.0) to the mineral medium. Each treatment was replicated six times.

The growth experiments were performed in 24-well microplates (Corning Incorporated, New York, NY, USA) placed in three sterilized 1.7 L glass incubation chambers, which in turn were placed in a large Orbital incubator (Gallenkamp, Leicester, UK) that was maintained at 25°C and provided 120 rpm shaking and light from TL-D 30W/33-640 white fluorescent tubes (Philips, Eindhoven, the Netherlands). The photon flux density at the wells, measured with an LI-250 light meter (LI-COR Biosciences, Lincoln, NE, USA), was 14-16 mmol photons m^{-2} s^{-1}. The mineral medium was a modified BG11 medium (Rippka *et al.*, 1979) with 5 mmol L^{-1} $NaNO_3$ and 5 mmol L^{-1} NaCl, but without addition of $NaHCO_3$ or Na_2CO_3 ('BG11*'). The glass incubation chambers were provided with CO_2-enriched air at a flow rate of 25 L h^{-1}. The CO_2-enriched air was based on CO_2-depleted pressurized air (21% O_2, 78% N_2; CO_2 was removed by two 1 m high columns filled with NaOH pellets) to which different amounts of pure CO_2 gas were added, using the GT 1355R-2-15-A 316 SS Flow Controllers and 5850S Mass Flow Controllers (Brooks Instrument, Hatfield, PA, USA). The gas mixture was moistened with 25°C water to suppress evaporation from the wells and led through a 0.20 mm Midisart 2000 filter (Sartorius Stedim Biotech GmbH, Göttingen, Germany) to sterilize the air, before it entered the incubation chambers. The CO_2 concentration in the gas mixture was checked regularly with an Environmental Gas Monitor for CO_2 (EGM-4; PP Systems, Amesbury, MA, USA).

At the start of the experiments, exponentially growing pre-cultures were diluted with BG11* to a similar absorbance at 750 nm of A_{750}≈0.015. The strains were randomized over the microplates to minimize position effects. The total start volume per well was 2,200 µL. Samples of 100 µL were taken from the wells on an almost daily basis for at least 1 week and transferred in a sterile fume hood to 96-well microplates (Corning Incorporated) to measure the A_{750} with a tunable Versamax microplate reader (Molecular Devices, Sunnyvale, CA, USA). A few wells close to the gas inlet of the incubation chambers showed substantial evaporation and were excluded from the data analyses. Specific growth rates were calculated from 3-5 time points during the exponential growth phase, as the slope obtained by linear regression of the natural logarithm of A_{750} versus time.

We ran an additional experiment with larger sixwell microplates (Corning Incorporated), using the same experimental conditions, to gather sufficient sampling volume to characterize the C_i conditions induced by the treatments. We used three wells per treatment. The wells were inoculated with one representative strain, *Microcystis* PCC 7005, at A_{750}≈0.015, and sampled one day after inoculation. The pH in the wells was measured with a Lab 860pH meter in combination with a BlueLine 28 Gel pH electrode (SCHOTT Instruments GmbH, Mainz, Germany). The well contents of the three biological replicates were combined, centrifuged at 4,000 *g* for 10 min at 20°C and filtered over 0.45 mm membrane filters (Whatman, Maidstone, UK) to determine the DIC concentration with a TOC-VCPH analyzer (Shimadzu, Kyoto, Japan) using 3-5 technical replicates per analysis. Concentrations of dissolved CO_2 (aq), bicarbonate and carbonate were calculated from DIC and pH (Stumm and Morgan, 1996).

Growth data of each *Microcystis* strain were analyzed with a two-way analysis of variance to test whether the specific growth rates were affected by the CO_2 level in the gas flow and the alkaline buffer in the mineral medium. We used Type III Sum of Squares to account for unequal sample sizes and the presence of significant interaction terms. *Post hoc* comparisons of the means were based on Tukey's unequal N HSD test, using a significance level α of 0.001.

Acknowledgements

We thank the three anonymous reviewers for their helpful comments, and Leo Hoitinga for assistance with the DIC measurements. This research was supported by the Earth and Life Sciences Foundation (ALW), which is subsidized by the Netherlands Organization for Scientific Research (NWO).

Supplementary Information

Contents

This section contains the following data:

I. Primers developed in this study
II. Alignment of LysR-type transcriptional regulators
III. Analysis of operon structure and transcription of CCM genes
IV. Statistical analysis of growth experiments

I. Primers developed in this study

Table S2.1. Overview of the *Microcystis* primers developed in this study for PCR analyses.

Primer name (primer number)	Sequence (5'→ 3')	Gene symbol	Function of complete protein/ complex	Locus tag	Accession no. (Genbank)	Reference
ccmR2-F1 (1)	TTTTCTCGACCATGGCATCAC	*ccmR2*	LysR-family transcriptional regulator of sodium-dependent bicarbonate uptake operon	*MAE_62070*	AP009552.1	This study
ccmR2-R1 (2)	TCCTTGGGATAAACCACATACCA					This study
ccmR2-R2 (3)	CAGTTGTTTCATCTGGGTGGA					This study
bicA-F1 (4)	CTGGCTTTATGTCTGGGATCG	*bicA*	Low-affinity bicarbonate/ sodium symporter	*MIC_4911*	AM778949.1	This study
bicA-F2 (5)	ATTGCCCTAAAAGTGGGGAT					This study
bicA-F3 (6)	CTGGCTTTATGTC**N**GGGAT**Y**G					This study
bicA-R1 (7)	CGATCCCAGACATAAAGCCAG					This study
bicA-R2 (8)	ATCCCCACTTTTAGGGCAAT					This study
bicA-R3 (9)	ATCCCCAC**Y**TT**D**AGGGCAAT					This study
bicAfrag-F4 (10)	CGTTTCTCTCCCTCTAGCTCTC	*bicA* + *bicA* frag-ment	Low-affinity bicarbonate/ sodium symporter	*MAE_62080*	AP009552.1	This study
bicAfrag-R4 (11)	TCGGGATTTTTGGCGGTTAAAC					This study
bicAfrag-F5 (12)	CTTGACGCTGTCCAAAGTTCTG					This study
sbtA-F1 (13)	GATCATCGTCTTCATGCTGCT	*sbtA*	High-affinity bicarbonate/ sodium symporter	*MAE_62090*	AP009552.1	This study
sbtA-F2 (14)	TTCGGTCTCGGCATGATTG					This study
sbtA-F3 (15)	CAACACTGGCCTTTTTGATTGG					This study
sbtA-R1 (16)	AGCAGCATGAAGACGATGATC					This study
sbtA-R2 (17)	AATCATGCCGAGACCGAAG					This study
sbtB-F1 (18)	AAGCTCGTCATCGTCACAGAA	*sbtB*	Linked with SbtA, function unknown	*MAE_62100*	AP009552.1	This study
sbtB-R1 (19)	ACGTTGCGACTGCCTTTAC					This study
nhaS3-R1 (20)	CTTCGAGGTAATACCGATACTGGT	*nhaS3*	Sodium/proton antiporter	*MAE_62110*	AP009552.1	This study
cmpA-F1 (21)	CGGTAGCGTTTCCTATCCCT	*cmpA*	High-affinity ATP-dependent bicarbonate uptake system	*MAE_19990*	AP009552.1	This study
cmpA-R1 (22)	TCCAAAGATCCTCGCGGTTA					This study
cmpB-F1 (23)	CTCGATCGCTTTATGGCTTGG	*cmpB*		*MAE_20000*	AP009552.1	This study
cmpC-R1 (24)	ACCGTTACGAGTCATAGTCAGG	*cmpC*		*MAE_20010*	AP009552.1	This study
cmpD-R1 (25)	GTGGGTAATCATCAACACCGTAC	*cmpD*		*MAE_20020*	AP009552.1	This study
ccmR-F1 (26)	CCTACCGTCTCAACCCAAGT	*ccmR*	LysR-family transcriptional regulator of the high-affinity CO_2 uptake operon	*MAE_15110*	AP009552.1	This study
ccmR-R1 (27)	ACAGTAATTCCTGACCCGCTT					This study
ndhF3-F1 (28)	CTGGGAGTGGCTTTTCTCTTG	*ndhF3*	High-affinity CO_2 uptake system	*MAE_15120*	AP009552.1	This study
ndhF3-R1 (29)	AGGTCGTTGGCAAAGAAATCTTG					This study

Table S2.1 continued.

ecaB-F1 (30)	TCAATACCTCTCGTCGCCAA	*ecaB*	β-type carbonic anhydrase	*MAE_15130*	AP009552.1	This study
ecaB-R1 (31)	CCTGGTCTGGGTTCAATCCT					This study
ndhD3-F1 (32)	TCCATACTTGGCTACCGGAT	*ndhD3*	High-affinity CO_2 uptake system	*MAE_15140*	AP009552.1	This study
ndhD3-R1 (33)	TGCAGACCAAAGCGAACTAAG					This study
chpY-F1 (34)	ATATCGCCAAAATGCCGACC	*chpY*	High-affinity CO_2 uptake system	*MAE_15160*	AP009552.1	This study
chpY-R1 (35)	GACATCATCCGCACCTGTTC					This study
chpX-F1 (36)	TCGAGGTAGTGGGTATCCTG	*chpX*	Low-affinity CO_2 uptake system	*MAE_35770*	AP009552.1	This study
chpX-R1 (37)	GTGGTAGTTAAAGGGTAAGGTGC					This study
ndhD4-F1 (38)	ATACTGATTGCCTACACGCCT	*ndhD4*	Low-affinity CO_2 uptake system	*MAE_58400*	AP009552.1	This study
ndhD4-R1 (39)	CCCGTGATTGGTAAACCTCTTTC					This study
ndhF4-F1 (40)	CAGTCTCTTGGCCCAAATCTATG	*ndhF4*	Low-affinity CO_2 uptake system	*MAE_27290*	AP009552.1	This study
ndhF4-R1 (41)	GTGAGAATTAAGGCTCCTGCG					This study
ecaA-F1 (42)	CCCAAGAACCTTCTCCTGAAATG	*ecaA*	α-type carbonic anhydrase	*MAE_14310*	AP009552.1	This study
ecaA-F1 (43)	GCCAATTGTTGCAGTTGTTGG					This study
ccaA1-F1 (44)	ACTCCTGCGGTTAATACTGTGG	*ccaA1*	Carboxysome carbonic anhydrase	*MAE_36580*	AP009552.1	This study
ccaA1-R1 (45)	GATAAATGCGATCAGCTTGGGAG					This study
ccaA2-F1 (46)	ATTCGTTCCCGATTACATCAAGG	*ccaA2*	Carboxysome carbonic anhydrase	*MAE_36560*	AP009552.1	This study
ccaA2-R1 (47)	AAGTTGCTCAACGGGATCG					This study
ccmM-F1 (48)	AAGTCCACACCTTCTCTAACCTC	*ccmM*	Carboxysome structural protein	*MAE_47910*	AP009552.1	This study
ccmM-R1 (49)	CTGTCGTCGCCAATGTGAA					This study
rpoC1-F1 (50)	TCCTCAGCGAAGATCAATGGT	*rpoC1*	RNA polymerase (γ subunit)	*MAE_11110*	AP009552.1	This study
rpoC1-R1 (51)	GTCTTTCCGCTTCTTCTTCCAG					This study
mcyB-F1 (52)	ATCCCATGCTCAGAGACGTT	*mcyB*	Microcystin synthetase gene	*MAE_38560*	AP009552.1	This study
mcyB-R1 (53)	AGATGTCCGCAGGGATTCAT					This study
mcyE-F1 (54)	CGCTCAACCGGCTATATTCG	*mcyE*	Microcystin synthetase gene	*MAE_38610*	AP009552.1	This study
mcyE-R1 (55)	TCCTGCGATACAAGCTGCTA					This study

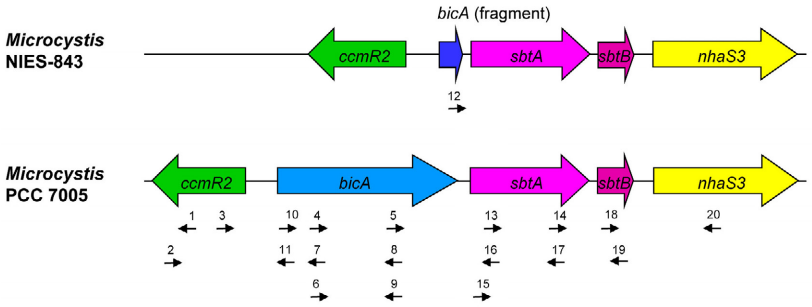

Figure S2.1. Graphical overview of the primers developed in this study for PCR-based detection of the *ccmR2*, *bicA*, *sbtAB* and *nhaS3* genes of *Microcystis*. The primers are numbered, and the corresponding primer sequences are enlisted in Table S2.1, Supplementary Information.

II. Alignment of LysR-type transcriptional regulators

We found three CcmR-like LysR transcriptional regulators in *Microcystis*:

1. The LysR transcriptional regulator gene *ccmR* has also been found in several other cyanobacteria (*e.g.*, Woodger *et al.*, 2007). In *Microcystis*, CcmR most likely regulates the high-affinity CO_2 operon (see section III of the Supplementary Information for the operon structure).
2. The additional LysR-type transcriptional regulator, CcmR2, most likely regulates transcription of the sodium-dependent bicarbonate uptake genes located in the *bicA-sbtAB-nhaS3* operon of *Microcystis*.
3. A third LysR-type transcriptional regulator, CbbR, most likely regulates expression of the RubisCO and Calvin-Benson cycle genes.

All 20 *Microcystis* strains that we investigated lacked the CmpR transcriptional regulator of the *cmpABCD* operon (encoding BCT1), although this regulator is known from several other cyanobacteria (*e.g.*, *Synechocystis* PCC 6803).

Alignment of the amino acid sequences revealed high similarities between the different CcmR-like transcriptional regulators of *Microcystis* (**Figure S2.2, Supplementary Information**). CcmR and CbbR were strongly conserved between the different *Microcystis* strains, with identical protein lengths. The additional LysR transcriptional regulator, CcmR2, is very similar to CcmR found in *Microcystis* and other cyanobacteria, and to CmpR of *Synechocystis* PCC 6803. However, CcmR2 showed more variation between different *Microcystis* strains than CcmR and CbbR, especially at the C-terminus (**Figure S2.2, Supplementary Information**). We did not find a relation between the C_i uptake genotypes and the sequence of CcmR2.

Figure S2.2 Alignment of the amino acid sequences of CcmR-like LysR transcriptional regulators of the 13 *Microcystis* strains of which the genome sequence was available, with *Synechocystis* PCC 6803 and *Synechococcus* PCC 7002 as reference species. CcmR and CbbR are shown only for *Microcystis* strains NIES-843 and PCC 7806, because these proteins were very similar in all 13 *Microcystis* strains. CcmR is shown for all 13 *Microcystis* strains, as there was more variation between different strains for this protein. The amino acid sequences were aligned with ClustalW version 2.1 (Thompson *et al.*, 1994) and visualized with Jalview version 2.7 (Waterhouse *et al.*, 2009). Residues are colored according to their physicochemical properties (using the Zappo colour scheme of Jalview).

III. Analysis of operon structure and transcription of CCM genes

Introduction

Our sequence analysis shows that the two sodium-dependent bicarbonate uptake genes *bicA* and *sbtAB*, and the sodium/proton antiporter gene *nhaS3* are all located next to each other in the genome of *Microcystis* (**Figure 2.1** of the main text). This suggests combined transcriptional regulation. In this section, we investigate transcription of the CCM genes to confirm gene expression and to unravel the operon structure of this genomic region as well as several other CCM operons of *Microcystis*.

Materials and Methods

To assess transcription of the CCM genes, four *Microcystis* strains (NIES-843, NIVA-CYA 140, PCC 7005 and PCC 7806) representing different C_i uptake genotypes were grown in batch culture provided with 400 ppm CO_2 for 5 days. Subsequently, the batch cultures were sparged with only 20 ppm CO_2 for 1 h to induce low C_i conditions. The batch cultures were run in 500 mL Erlenmeyer flasks shaken at 120 rpm at 25°C and continuous light of 15 µmol photons m^{-2} s^{-1} (15W F15T8 white fluorescent tubes; GE Healthcare, Piscataway, NJ, USA), using the modified BG11* medium described in the Materials and Methods of the main text.

Before and after sparging with 20 ppm CO_2, samples of 80 mL were taken for RNA isolation. Cells were rapidly cooled with ice and pelleted by centrifugation at 4°C (4,000 *g*, 10 min). The pellets were resuspended in 1 mL TRIzol (Invitrogen GmbH, Karlsruhe, Germany) and immediately frozen in liquid N_2. The samples were then either stored at -80 °C for later processing or processed immediately. RNA isolation with TRIzol (Invitrogen) was done according to the supplier's instructions, using beads (0.5 mm BashingBeads; Zymo Research, Orange, CA, USA) to facilitate cell disruption. After the phase separation steps, the Direct-Zol™ RNA MiniPrep kit (Zymo Research) was used for RNA purification. The in-column DNase I digestion was included as well. The purity of the isolated RNA was analyzed afterwards with a Nanodrop 1000 spectrophotometer (Thermo Scientific, San Jose, CA, USA) and only samples with A_{260}/A_{280} and A_{260}/A_{230} values above 1.8 were used for subsequent cDNA synthesis. 5 µg of pure RNA was used for cDNA synthesis with Superscript III (Invitrogen) according to the supplier's instructions. Reactions without reverse transcriptase enzyme were used as well to test for possible DNA contamination of the samples.

PCR reactions were done on the cDNA with GoTaq® DNA polymerase, as described in the main text, using combinations of specific primers targeting several CCM genes (**Figure S2.1**, **Table S2.1, Supplementary Information**). Subsequently, gel electrophoresis was used to analyze the PCR products and to confirm the presence or absence of specific transcripts. To unravel the operon structures of the CCM genes, the observed PCR product lengths were

compared with the expected PCR product lengths assuming that the target genes were co-transcribed. If the expected and observed PCR product lengths match, the target genes are most likely in the same operon.

Results

The transcriptional analysis detected expression of all five different C_i uptake genes and all four CA genes (**Tables S2.2 and S2.3, Supplementary Information**). Controls without added reverse transcriptase enzyme were negative, indicating that the RNA samples were DNA-free (**Tables S2.2 and S2.3, Supplementary Information**). Furthermore, gene expression was lacking when the gene was not in the genome of the strain concerned, which demonstrates the consistency of the results. Most gene products were detected both before and after sparging with 20 ppm CO_2. However, *cmpA* transcripts of strain NIES-843 were detected only in samples taken after sparging with 20 ppm CO_2 (**Table S2.3, Supplementary Information**), probably due to induction of the high-affinity bicarbonate uptake system BCT1 at low CO_2 levels (Omata *et al.*, 1999).

In strain PCC 7005, *bicA*, *sbtAB* and *nhaS3* were co-transcribed (**Table S2.2, Supplementary Information**). Strain PCC 7806 lacked the *sbtAB* genes (**Figure 2.1**), but co-transcribed *bicA* and *nhaS3* (**Table S2.2, Supplementary Information**). Strain NIES-843 had a *bicA* fragment adjacent to *sbtAB*, and it co-transcribed this *bicA* fragment, *sbtAB* and *nhaS3* (**Table S2.2, Supplementary Information**). Hence, the *bicA* promoter was still used, which might be the reason why the *bicA* fragment has not been lost entirely. In strain NIVA-CYA 140, which had a transposon inserted within a complete *bicA* gene (**Figure 2.1**), co-transcripts were detected with a forward primer around the 3'-end of *bicA* and a reverse primer on *sbtA*, *sbtB* or *nhaS3* (**Table S2.2, Supplementary Information**). However, PCR reactions with a forward primer around the 5'-end of *bicA* and a reverse primer near the 3'-end of *bicA* yielded no product, which is likely caused by the transposon complicating the reverse transcription and/or PCR. In total, these patterns of co-transcription provide strong evidence that, in *Microcystis*, the genes *bicA* (or its fragment), *sbtAB* (when present) and *nhaS3* are located on the same operon.

In *Microcystis*, and many other cyanobacteria, the ATP-dependent bicarbonate uptake system BCT1 is encoded by the *cmpABCD* operon. In addition, the high-affinity CO_2 genes *ndhF3*, *ndhD3* and *chpY*, the transcriptional regulator gene *ccmR* and the carbonic anhydrase gene *ecaB*, appeared to be part of one operon as well, with the following operon structure: *ccmR-ndhF3-ecaB-ndhD3-chpY* (**Table S2.3, Supplementary Information**). In contrast, the genome sequences of all 13 sequenced *Microcystis* strains showed that the low-affinity CO_2

uptake genes *ndhD4*, *ndhF4* and *chpX* are not in one operon but at separate locations in the genome.

Sequence alignments were made of the transcriptional start sites (TSSs) of the investigated CCM genes/operons of different *Microcytis* strains (data not shown). Possible LysR CcmR/CcmR2 binding sites were found near the most likely -10 TSS of the *cmpABCD* operon, high-affinity CO_2 operon and sodium-dependent bicarbonate uptake operon, indicating that the expression of these sets of C_i uptake genes is most likely strongly regulated.

Table S2.2. Transcriptional analysis of the genes *ccmR*, *bicA*, *sbtA* and *nhaS3* in four *Microcystis* strains.

	Target genes	Primers	Expected PCR product length (bp)	Observed PCR product length (bp)			
				NIES-843	NIVA-CYA 140	PCC 7005	PCC 7806
+RT	*ccmR2*	1+2	204	204	204	204	204
	bicA	4+8	682/1903	–	–	682	682
	bicA(fragment)	10+11	84/195	84	195	195	195
	sbtA	13+17	849	849	849	849	–
	bicA(fragment)-*nhaS3*	10+20	2346/2512/ 4026/5247	2512	–	4026	2346
	bicA(fragment)-*sbtA*	10+17	1146/2653/3874	1146	–	2653	–
	bicA(fragment)-*sbtB*	10+19	1576/3092/4313	1576	–	3092	–
	bicA(end)-*sbtA*	5+16	934	–	934	934	–
	sbtA-*sbtB*	14+19	450	450	450	450	–
	sbtA-*nhaS3*	14+20	1386-1393	±1390	±1390	±1390	–
-RT	*bicA*	4+8	682/1903	–	–	–	–
	sbtA	13+17	849	–	–	–	–

The table compares the observed PCR product lengths of the *Microcystis* strains with the expected PCR product length assuming that the enlisted target genes are co-transcribed. The observed PCR products were obtained from PCR reactions on cDNA reverse transcribed from RNA of the target genes. If the expected and observed PCR product lengths match, the target genes are most likely in the same operon. Dash signs (–) indicate the lack of a PCR product. The primer sequences are provided in Table S2.1, Supplementary Information.

+RT, cDNA produced by reverse transcriptase; -RT, controls without reverse transcriptase.

Table S2.3. Transcriptional analyses of CCM genes in four *Microcystis* strains.

	Target genes	Primers	Expected PCR product length (bp)	Observed PCR product length (bp)			
				NIES-843	NIVA-CYA 140	PCC 7005	PCC 7806
+RT	*rpoC1*	50+51	144	144	144	144	144
	cmpA	21+22	137	137*	137	137	137
	ccmR	26+27	109	109	109	109	109
	ccmR-ndhF3	26+29	2487	2487*	2487	2487	2487
	ccmR-ecaB	26+31	2998-2999	–	±2999	±2999	±2999
	ndhF3-ndhD3	28+33	2061-2063	±2062	±2062	±2062	±2062
	ecaB-ndhD3	30+33	1578-1579	±1579	±1579	±1579	±1579
	ecaB-chpY	30+35	3016/3233	–	3016	3016	3016
	ndhD4	38+39	1070	1070	1070	1070	1070
	ndhF4	40+41	774	774	774	774	774
	chpX	36+37	937	937	937	937	937
	ecaA	42+43	187	187	187	187	187
	ccaA1	44+45	97	97	97	97	97
	ccaA2	46+47	137	137	–	–	–
	ccmM	48+49	118	118	118	118	118
-RT	*rpoC1*	50+51	144	–	–	–	–

The table compares the observed PCR product lengths of the *Microcystis* strains with the expected PCR product length assuming that the enlisted target genes are co-transcribed. The observed PCR products were obtained from PCR reactions on cDNA reverse transcribed from RNA of the target genes. If the expected and observed PCR product lengths match, the target genes are most likely in the same operon. +RT, cDNA produced by reverse transcriptase; -RT, controls without reverse transcriptase. Dash signs (–) indicate the lack of a PCR product. Results marked with an asterisk (*) indicate PCR products that were detected only in samples taken after sparging with 20 ppm CO_2. The RNA polymerase gene *rpoC1* was used as a control. The primer sequences are provided in Table S2.1, Supplementary Information. Results for the sodium-dependent bicarbonate uptake genes *bicA* and *sbtA* are reported in Table S2.2, Supplementary Information.

IV. Statistical analysis of growth experiments

We tested whether the specific growth rates of the four *Microcystis* strains investigated in the growth experiments were affected by the CO_2 level in the gas flow and the alkaline buffer in the mineral medium. The Shapiro-Wilks test indicated that the specific growth rates did not follow a normal distribution, even after log-transformation. However, analysis of variance (ANOVA) is relatively robust against violations of the normal distribution assumption (Schmider *et al.*, 2010). We therefore applied a two-way ANOVA for each *Microcystis* strain, with specific growth rate as the dependent variable and the CO_2 concentration in the gas flow (pCO_2) and the presence of alkaline buffer in the mineral medium as independent variables. All treatments were replicated six times. However, some of the wells close to the gas inlet of the incubation chambers showed substantial evaporation, and were excluded from the data analyses. We therefore used Type III Sum of Squares to account for unequal samples sizes. *Post-hoc* comparisons of the means were based on Tukey's unequal N HSD test, using a significance level α of 0.001.

The results of the two-way ANOVA show significant main effects of pCO_2 and buffer and a significant interaction term for strain PCC 7806, its non-toxic mutant PCC 7806 Δ*mcyB*, and strain NIES-843 (**Table S2.4, Supplementary Information**). In contrast, the specific growth rate of strain PCC 7005, which contains both *bicA* and *sbtA*, was not significantly affected by the treatments. The results of the *post-hoc* comparison of the means are presented in **Figure 2.4** of the main text, and further interpretation of these statistical results is postponed to the main text.

Table S2.4. Results of the two-way ANOVA, with the specific growth rate of the *Microcystis* strain as the dependent variable, and CO_2 concentration (pCO_2) and alkaline buffer as independent variables.

Effect	df_1, df_2	F	P
Microcystis PCC 7806			
pCO_2	2, 26	439.49	<0.001
buffer	1, 26	191.50	<0.001
pCO_2 × buffer	2, 26	110.46	<0.001
Microcystis PCC 7806 Δ*mcyB*			
pCO_2	2, 24	212.15	<0.001
buffer	1, 24	39.32	<0.001
pCO_2 × buffer	2, 24	19.34	<0.001
Microcystis PCC 7005			
pCO_2	2, 24	1.21	0.316
buffer	1, 24	2.32	0.141
pCO_2 × buffer	2, 24	2.55	0.099
Microcystis NIES-843			
pCO_2	2, 24	87.27	<0.001
buffer	1, 24	6.31	0.019
pCO_2 × buffer	2, 24	14.63	<0.001

Columns indicate the variables of interest, the main effects and interaction effects, the degrees of freedom (df_1 *and* df_2), the value of the *F*-statistic ($F_{df1,df2}$) and the corresponding probability (*P*).